SALAH EL-DIN EL-MORSEDY

[Left hand page running head is author's name in Times New Roman 8 point bold capitals, centred. For more than two authors, write **AUTHOR et al.**]

CONFERENCE PRE-PRINT

STUDY ON THE THERMAL PERFORMANCE OF ITER TUNGSTEN DIVERTOR MONOBLOCK USING NANOFLUID FOR COOLING ENHANCEMENT

SALAH EL-DI.N EL-MORSHEDY Egyptian Atomic Energy Authority Cairo, Egypt Email: s.e.elmorshedy@gmail.com

Abstract

Due to its position and functions, the divertor has to sustain very high heat flux arising from the plasma (up to 20 MW/m²), while experiencing an intense nuclear deposited power, which could jeopardize its structure and limit its lifetime. Therefore, attention has to be paid to the thermal-hydraulic design of its cooling system. It is necessary to take effective cooling methods from the divertor which can sustain very high heat fluxes. Nanofluids have gained extensive attention due to their role in improving the efficiency of thermal systems. Recently, a further enhancement is achieved in heat transfer coefficients in combination with the addition of swirl-tape inserts. In a previous work, the author developed a mathematical model to investigate the steady state and transient thermal–hydraulic performance of ITER tungsten divertor monoblock. The model could predict the thermal response of the divertor structural materials for bare cooling tube and a cooling tube with swirl-tape inserts. In this work, the previous model has been updated to investigate the thermal performance of the ITER tungsten divertor monoblock using the nanofluid heat transfer enhancement technique. A water based TiO₂ nanofluid at 3% concentrations is used to cool the divertor. The model is then used to predict the steady state thermal behaviour of the divertor under incident surface heat fluxes ranges from 2 to 20 MW/m² for a bare and swirl-tape inserts divertor tube cooled by water and nanofluid. The results showing a considerable enhancement in the heat transfer process in the diveror of swirl-tape tube cooled by nanofluid.

1. INTRODUCTION

In fusion tokamak reactors, such as the International Thermonuclear Experimental Reactor (ITER) [1], the plasma facing components (PFCs) are exposed to one sided heat fluxes that are created by energetically charged particles and photons striking the PFC surfaces. The divertor target plates are the most thermally loaded invessel components in a fusion reactor where high heat fluxes are produced on the PFCs by intense plasma bombardment, radiation and nuclear heating by neutron irradiation. PFCs are designed to withstand the highest surface heat fluxes, i.e. 10 MW/m² during steady state operation and 20 MW/m² during slow transients [2]. In order to meet these requirements, the PFCs employ a monoblock technology, made of pure tungsten armour joined to the copper alloy pipe via a pure copper interlayer [3.4]. Due to the extremely high heat flux values in fusion reactors, a heat transfer enhancement technique is required in order to achieve a sufficient margin on critical heat flux at a reasonable flow velocity. The usage of swirl-tape insrts in flow boiling experiments were performed in 1962 [5] for pressurized water reactor studies at Argonne National Laboratory. This and subsequent research reveal that swirl-tape inserts in the coolant channels significantly increase the heat transfer coefficient in forced convection regime [6]. The swirl-tape inserts influence on the fully developed nucleate boiling regime is negligible; however, they considerably increase the critical heat flux [7]. Liu et al [8] examined the heat transfer enhancements of the subcooled flow boiling in the vertically upward screw tubes, the tubes with swirl-tape inserts and the plain tubes by the Fluent software. In order to remove high heat fluxes for plasma facing components in ITER divertor, a numerical simulation of subcooled water flow boiling heat transfer in a vertically upward smooth tube was conducted on the condition of one-sided high heat fluxes [9]. Numerical results indicate that the onset of nucleate boiling and fully developed boiling appear earlier and earlier with increasing heat flux. With the increase of heat fluxes, the inner CuCrZr tube will deteriorate earlier than the outer tungsten layer and the middle oxygen-free high-conductivity copper layer. Nanofluids have also gained extensive attention due to their role in improving the efficiency of thermal systems. A further enhancement in heat transfer coefficients was reported in combination with structural modifications of flow systems namely, the addition of swirl-tape inserts. Experiments are undertaken to determine heat transfer coefficients and friction factor of TiO₂/water nanofluid up to 3.0% volume concentration at an average temperature of 30°C [10]. The investigations are undertaken in the Reynolds number range of 8000-30,000 for flow in tubes and with swirl-tape inserts of different swirl-tape ratios. A significant enhancement of 23.2% in the heat transfer coefficients is observed at 1.0% concentration for f low in a tube. With the use of swirl-tape inserts, the heat transfer coefficient increased with decrease in swirl-tape ratio for water and nanofluid. The heat transfer coefficient and friction factor are respectively 81.1% and 1.5 times greater at Re^{1/4} 23,558 with 1.0% concentration and swirl-tape ratio of 5, compared to values with flow of water in a tube. Azmi et al [11] investigated experimentally the heat transfer coefficient and friction factor of TiO2 and SiO2 water based nanofluids flowing in a circular tube under turbulent flow under constant heat flux boundary condition. TiO2 and SiO₂ nanofluids with an average particle size of 50 nm and 22 nm respectively were used in the working fluid for volume concentrations up to 3.0%. Experiments were conducted at a bulk temperature of 30°C in the turbulent Reynolds number range of 5000 to 25,000. The enhancements in viscosity and thermal conductivity of TiO₂ are greater than SiO₂ nanofluid. However, a maximum enhancement of 26% in heat transfer coefficients is obtained with TiO2 nanofluid at 1.0% concentration, while SiO2 nanofluid gave 33% enhancement at 3.0% concentration. Sundar et al [12] conducted experiments in the particle volume concentration range of $0 < \phi <$ 0.6%, swirl-tape inserts of swirl-tape ratio in the range of 0 < Y < 15 and Reynolds number range of 3000 < Re< 22000. Heat transfer and friction factor enhancement of 0.6% volume concentration of Fe3O4 nanofluid in a plain tube with swirl-tape inserts of Y = 5 is 51.88% and 1.231 times compared to water flowing in a plain tube under same Reynolds number. Safikhani and Eiamsa-ard [13] used experimentally derived correlations of heat transfer and pressure drop in a Pareto based Multi-Objective Optimization (MOO) approach to find the best possible combinations of heat transfer and pressure drop of TiO₂-water nanofluid flow in tubes fitted with multiple swirl-tape inserts in different arrangement. El-Morshedy and Hassanein [14,15], developed a computer code entitled ITERTHA to simulate the cooling processes of a flat tile divertor in both normal and off-normal operation. Later on, El-Morshedy [16] updates this model to investigate the steady-state and transient thermal-hydraulic performance of ITER tungsten divertor monoblock. The model predicts the thermal response of the divertor structural materials and coolant tube. The model also accounts for the melting, vaporization, and re-solidification of the upper layer of the divertor facing plasma. El-Morshedy [17] also used the new model to perform a thermal-hydraulic simulation and safety analysis on ITER tungsten divertor monoblock in order to predict the thermal response of its structural materials under loss of flow transient. This transient is initiated by a trip of the main pump during plasma burn at an incident heat flux of 10 MW/m² at the divertor surface and a coolant velocity of 16 m/s. The pump coast-down is represented by an exponential reduction in the coolant velocity with time constants of 5, 10, 15, 20 and 25 s that cover almost all possible pump coast-down flow. In the present work, the previous model [16] is modified and updated to investigate the thermal performance of the ITER tungsten divertor monoblock using water and nanofuild coolant for cooling enhancement in a divertor of bare and swirl-tape inserts tube.

2. METHODOLOGY

The heat generated in nuclear fusion reactors will be extracted by the first wall of the blanket and in the water-cooled divertor. It is intended to perform a heat collection without losses, which requires materials that can withstand intense neutron irradiation and very high heat fluxes, without compromising their physical integrity. The present design for the water-cooled divertor consists of tungsten monoblocks crossed by a CuCrZr pipe where the coolant circulates while pure copper is used as interlayer. Tungsten has chosen to be the Plasma Facing Material (PFM) for the divertor of ITER due to its high thermal conductivity, high melting point, low tritium inventory, etc. During the ITER operation, tungsten -based PFMs are foreseen to face severe heat loads generated by transient events such as plasma disruption, edge localized modes (ELMs), and vertical displacement events (VDEs) [18]. CuCrZr alloy has been selected as the baseline heat sink material owing to the excellent thermal conductivity and good mechanical properties. Such an ideal combination is the unique advantage of CuCrZr alloy adequate for high heat flux applications. The presence of the thick soft copper layer is widely thought to be needed to relax the residual stress after fabrication which would be otherwise quite high. Fig. 1 shows the dimensions of the ITER tungsten divertor monoblock.

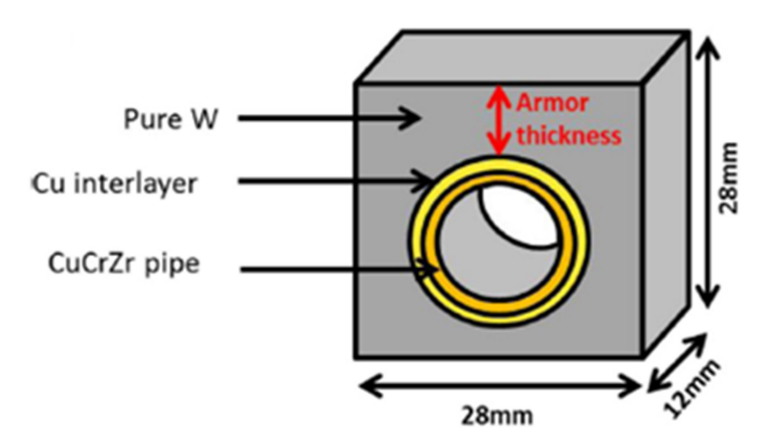


FIG. 1. ITER tungsten divertor monoblock scheme [19].

[Left hand page running head is author's name in Times New Roman 8 point bold capitals, centred. For more than two authors, write **AUTHOR et al.**]

The coolant tube is divided into a specified axial regions while the last radial surface of the divertor including the CuCrZr pipe and Cu interlayer is divided into a two-dimensional mesh in Cartesian coordinate system. Then nodal thermal-hydraulic calculations for coolant and divertor structure materials are performed with a uniform incident surface heat flux on the divertor upper surface.

2.1. Coolant temperature

The coolant is treated as one lumped node, thus it is assumed that the coolant is well stirred and has a uniform temperature. The coolant tube is divided into a given number of elements in the axial z-direction and the general energy balance equation is applied to each element:

$$\rho a \Delta z \frac{dI(\tau)}{d\tau} = \int_{0}^{2\pi} \phi(\tau, \theta) d\theta R \Delta z + G(\tau) A(I_{in}(\tau) - I_{out}(\tau))$$
(1)

where a is the channel cross-sectional area, $\phi(\tau,\theta)$ is the wall heat flux at time τ and radial angle θ , R is the coolant channel radius and $G(\tau)$ and $I(\tau)$ are the coolant mass and coolant enthalpy flux respectively at time τ .

2.2. Divertor temperature

The temperature distribution through the divertor is governed by the two-dimensional general heat conduction equation that takes the following form in Cartesian coordinates:

$$\rho c_p \frac{dt}{d\tau} = \frac{\partial}{\partial x} \left(k(t) \frac{\partial t}{\partial x} \right) + \frac{\partial}{\partial y} \left(k(t) \frac{\partial t}{\partial y} \right) + q(x, y, z)$$
(2)

The heat conduction in the mesh nodes of the divertor is solved in two-dimensions using the finite difference technique. Many governing equations are derived from the general conduction equation to cover all the mesh points.

2.3. Coefficient of heat transfer

The heat transfer coefficient is calculated for the single-phase or boiling two-phase flow where the flow regime is first identified at each axial node and then the heat transfer coefficient is estimated as follows:

2.3.1. Single-phase forced convection

(a) Turbulent regime Re ≥ 10,000; Dittus & Boelter [20] correlation is used:

$$Nu = 0.023 \,\mathrm{Re}^{0.8} \,\mathrm{Pr}^{0.4}$$
 (6)

- (b) Transition regime 2100 < Re < 10,000; Nusselt number is calculated by interpolation between the laminar and turbulent correlations.
- (c) Forced laminar regime $Re \le 2100$; Sieder & Tate [21] correlation is used:

$$Nu = 1.86 \left(\frac{\text{Re Pr}}{L/D_e} \right)^{1/3} \left(\frac{\mu_c}{\mu_w} \right)^{0.14}$$
 (7)

When cooling by nanofluid in a bare tube, the Nusselt number data of the nanofluids obtained from Maiga et al. [22] is subjected to non-linear regression analysis and the constant "a" is obtained as 0.085 for TiO₂/water nanofluid resulting in the following correlation:

$$Nu_{nf} = 0.085 \operatorname{Re}_{nf}^{0.71} \operatorname{Pr}_{nf}^{0.35} \tag{8}$$

When the cooling channel features a swirl-tape inserts, swirl-tape factors must be applied to the previously described heat transfer correlations that were defined for bare tubes [23]. The value of Nusselt number is multiplied by the swirl-tape modification of Lopina and Bergles [24] as follows:

$$Nu_{st} = Nu \times 2.26 \, Y^{-0.248} \tag{9}$$

where Y is the swirl-tape ratio, defined as the number of tube inner diameters per the pitch length for 180° rotation of the tape.

When cooling by TiO₂/water nanofluid with swirl-tape inserts, the following equation [10] is used:

$$Nu_{nf} = \frac{h_{nf}D}{k_{nf}} = 0.027 \,\mathrm{Re}^{0.693} \,\mathrm{Pr}_{nf}^{-0.3} \left(1 + \frac{1}{Y}\right)^{1.3}$$
 (10)

This equation is applicable for nanofluid up to 3.0% volume concentration. The equation was obtained with 321 data points with an average deviation of 4.5%, standard deviation of 5.7% and maximum deviation of 13.5%.

The density and specific heat of nanofluid are estimated by:

$$\rho_{nf} = \varphi \rho_n + (1 - \varphi) \rho_w \tag{11}$$

$$Cp_{nf} = \varphi Cp_p + (1 - \varphi)Cp_w \tag{12}$$

Timofeeva et al. [25] equation is used for computing the thermal conductivity of nanofluids:

$$k_{nf} = (1+3\varphi)k_{w} \tag{13}$$

The well-known Einstein's equation suggested by Drew and Passman [26] is used for calculating the viscosity, which is applicable to spherical particles in volume fractions less than 5.0 %:

$$\mu_{nf} = (1 + 2.5\varphi)\mu_{w} \tag{14}$$

2.3.2. Subcooled boiling

Boiling is initiated when the coolant channel surface temperature is equal to the onset of nucleate boiling temperature, T_{ONB}, where

$$t_{ONB} = t_{sat} + (\Delta t_{sat})_{ONB} \tag{15}$$

 $t_{ONB} = t_{sat} + (\Delta t_{sat})_{ONB}$ where $(\Delta t_{sat})_{ONB}$ is given by Bergles and Rohsenow correlation [27] which is valid for water only over the pressure range 1-138 bar:

$$\left(\Delta t_{sat}\right)_{ONB} = 0.556 \left(\frac{\phi_{ONB}}{1082P^{1.156}}\right)^{0.463\,P^{0.0234}} \tag{16}$$

where P is the local pressure in bar and ϕ_{ONB} is in W/m².

The inserted swirl-tape induces a secondary swirling flow, which causes ONB to occur at a higher heat flux condition than the smooth tube. As the swirl-tape ratio decreased, the ONB heat flux enhancement rate increased. Subcooling and mass flow rate have a proportional relationship with ONB heat flux, whereas pressure has an inverse relationship. Lim et al [28] correlation is used for the prediction of incipient nucleate boiling in a one-side heated swirl-tape inserts tube:

$$Bo_{ONB} = 0.036057 \times \text{Re}_{SW}^{-0.2773} \times Ja^{0.548} \times Rd^{0.0846} \times \left(1 + \frac{2.752}{Y^{1.29}}\right)$$
(17)

$$\frac{\left(\Delta t_{sat}\right)_{ONB}}{t_{sat}} = 0.112641 \times Bo^{0.4033} \times Rd^{-0.6136}$$
(18)

were
$$Bo = \frac{\phi}{G \times h_{fg}}$$
, $Re_{sw} = \frac{\rho V_{sw} D}{\mu} = Re \times \sqrt{1 + \left(\frac{\pi}{2Y}\right)^2}$, $Ja = \frac{Cp(T_{sat} - T_b)}{h_{fg}}$, and $Rd = \frac{\rho_g}{\rho_f}$.

The correlation developed by Chen [29] for saturated boiling is extended for use in the subcooled boiling. It is assumed that the total heat flux is made up of a nucleate boiling contribution and a single phase forced convective contribution

$$\phi(z) = h_{NCB} (t_w(z) - t_{sat}) + h_{SP} (t_w(z) - t_c(z))$$
(19)

where h_{SP} is calculated as described above in Section 2.3.1 and h_{NCB} is calculated for saturated boiling detailed in the next section.

$$h_{SP} = 0.023 \left(\frac{G(1-x)D_e}{\mu_l} \right)^{0.8} \left(\frac{\mu c_p}{k} \right)^{0.4} \left(\frac{k_l}{D_e} \right)$$
 (20)

$$h_{NCB} = 0.00122 \left(\frac{k_l^{0.79} c_{pl}^{0.45} \rho_l^{0.49}}{\sigma^{0.5} \mu_l^{0.29} I_{fg}^{0.24} \rho_g^{0.24}} \right) \Delta t_{sat}^{0.24} \Delta P_{sat}^{0.75} (S)$$
 (21)

where Δt_{sat} is the wall superheat, ΔP_{sat} is the difference between the saturation pressures calculated from the wall temperature and the fluid temperature and S is the nucleate boiling suppression factor and calculated as

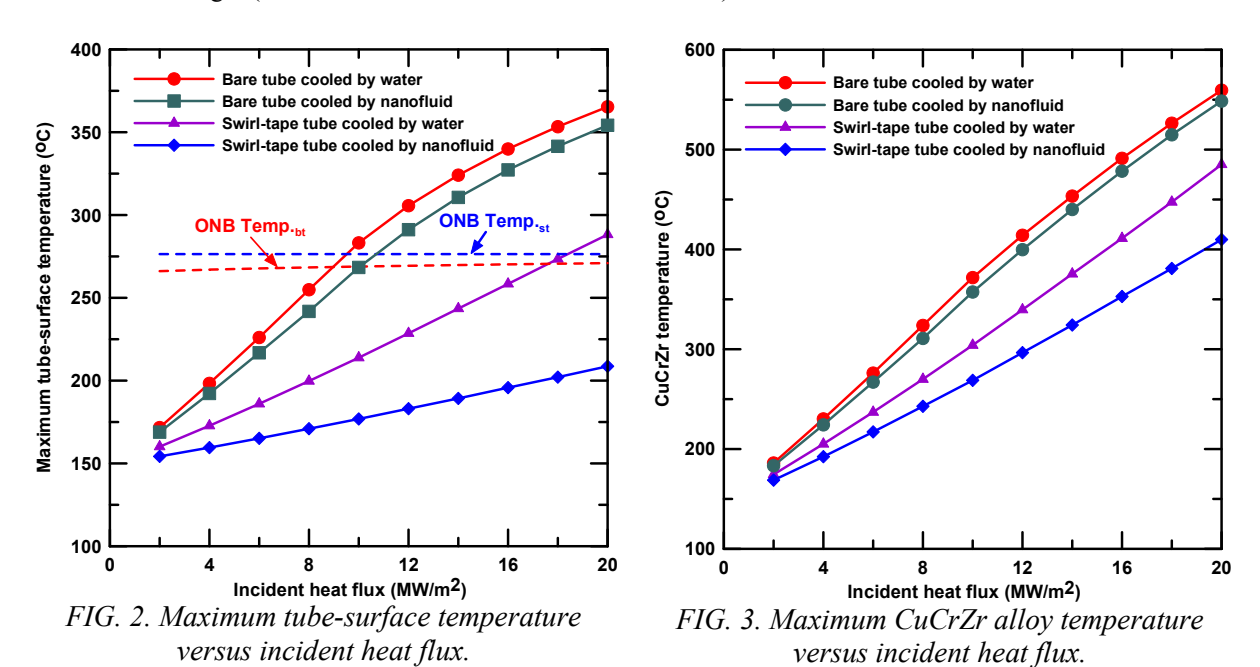
$$S = \begin{cases} \left(1 + 0.12 \operatorname{Re}_{TP}^{1.14}\right)^{-1} & for \quad \operatorname{Re}_{f} < 32.5\\ \left(1 + 0.42 \operatorname{Re}_{TP}^{0.78}\right)^{-1} & for \quad 32.5 < \operatorname{Re}_{f} < 70 \end{cases}$$
(22)

$$Re_f = \frac{GD}{\mu_f} \tag{23}$$

3. RESULTS

The incident heat on the divertor upper surface is deposited in the divertor structure and removed by a high water flow rate through the cooling tube. It is supposed that, the right, left and lower surfaces of the divertor module are under adiabatic conditions because the divertor is equipped in the plasma vessel. The operating conditions are; inlet temperature: 150°C, pressure: 5 MPa and coolant velocity: 16 m/s.

Up to now there is no fully consolidated quantitative prediction of the surface heat flux profile. Thus, the heat flux profile specified for the ITER divertor targets was adopted in WPDIV as a tentative specification where the peak heat flux was assumed to be 10 MW/m² for the quasistationary operation (2 h) and 20 MW/m² for slow transient events (< 10 s). Therefore; calculations are performed for incident surface heat flux of 2, 4, 6, 8, 10, 12, 14, 16, 18 and 20 MW/m² for a divertor cooled by (a) water through bare tube, (b) nanofluid through bare tube, (c) water through swirl-tape inserts tube and (d) nanofluid through swirl-tap inserts tube. The swirl-tape insertion is of ratio 2 and thickness 1 mm and a water based TiO₂ nanofluid at 3% concentrations is used. Fig. 2 shows the variation of the predicted maximum tube-surface temperature values versus the incident surface heat flux for the four cases as well as the onset of nucleate boiling temperatures for both bare and swirl-tape inserts tubes. It is found that, by replacing water by nanofluid in the bare tube diverter, the heat transfer coefficient is slightly enhanced. On the other hand, when using swirl-tape insertion a considerable enhancement in the heat transfer coefficient is obtained and this enhancement is considerably increased by the combination of swirl-tape inserts and nanofluid cooling. It is also found that, for bare tube divertor, the maximum tube surface temperature exceeds the ONB temperature for incident heat fluxes greater than 10 MW/m² and so subcooled boiling is predicted at the upper surface of the tube. While for swirl-tape inserts tube divertor, subcooled boiling is predicted at the upper surface of the tube for incident heat fluxes greater than 18 MW/m². This is attributed to the enhancement in the heat transfer coefficient due to swirl-tape insertion. It is noticed that, when replacing water coolant by nanofluid in the swirl-tape inserts tube divertor, the heat transfer process reveals much more enhancement and the tube-surface temperature remains below the onset of nucleate boiling temperature by a considerable margin (68°C at an incident heat flux of 20 MW/m²).



The maximum temperature values in CuCrZr alloy, Copper, and tungsten for the four cases are also depicted in Figs. 3, 4 and 5 respectively were its temperatures are decreased slightly by replacing water by nanofluid in the bare tube diverter. On the other hand, when using swirl-tape inserts tube divertor cooled by water, the temperatures are considerably decreased and decreased much more by using nanofluid and the temperature reduction rate is equal to the corresponding temperature reduction in the tube-surface temperature due the enhancement in the heat transfer coefficient.

It is also noticed that, the predicted maximum temperatures of the CuCrZr alloy exceed the upper allowable temperature limit (specified to be around 300-330°C considering irradiation creep [30,31]) for incident surface heat fluxes greater or equal to 10 MW/m² for bare tube divertor cooled by water or nanofluid and 12 MW/m² for swirl-tape inserts tube divertor cooled by water; while for swirl-tape inserts tube divertor cooled by

nanofluid, the upper temperature limit is exceeded at incident surface heat fluxes greater or equal to 18 MW/m^2 . However, these temperature values could be reduced by using a water-cooling at lower temperature.

Fig. 6 shows a contour plot of the temperature distribution through the swirl-tape inserts tube divertor cooled by both water and nanofluid at an incident surface heat flux of 20 MW/m². It shows clearly that, the temperature values are relatively lower for swirl-tape inserts tube divertor cooled by nanofluid than the corresponding values for water cooling due to the enhancement in the heat transfer process resulting from the combined effect of swirl-tape inserts and nanofluid cooling.

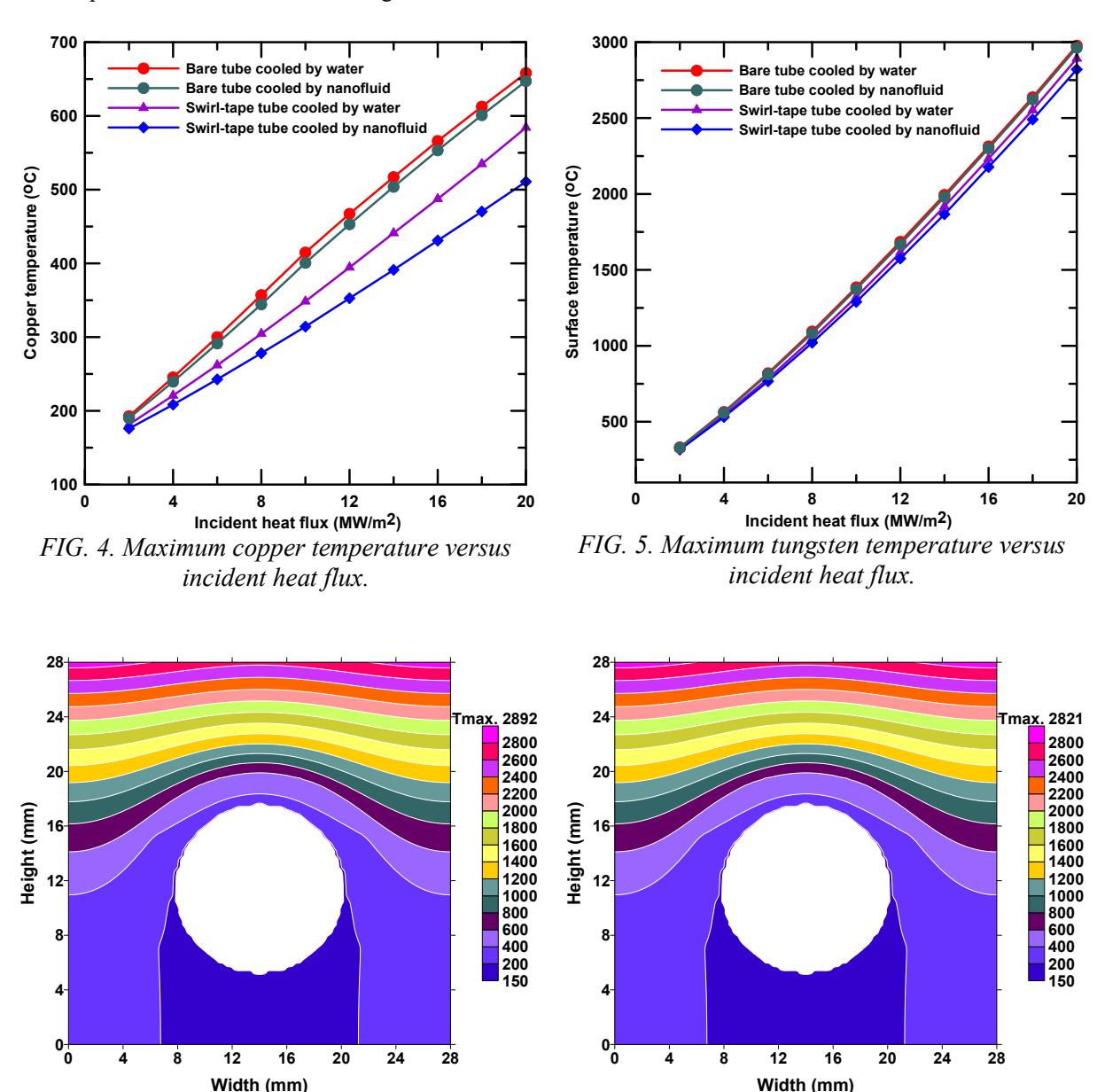


FIG. 6. Temperature distribution in the swirl-tape tube divertor at an incident heat flux of 20 MW/m².

(b) nanofluid cooling

4. CONCLUSION

(a) water cooling

A previously developed model for simulating the thermal-hydraulic response of ITER tungsten divertor mono block structural materials has been updated to simulate the divertor cooling by nanofluid for both bare and swirltape inserts tube. The selected heat transfer correlations cover all possible operating conditions of ITER for both normal and off-normal plasma events. The model is used to predict the temperature distribution through the divertor structure materials for incident surface heat flux values of 2, 4, 6, 8, 10, 12, 14, 16, 18 and 20 MW/m² for a divertor cooled by water through bare tube, nanofluid through bare tube, water through swirl-tape inserts tube and nanofluid through swirl-tape inserts tube. The swirl-tape insertion is of ratio 2 and thickness 1 mm and

a water based TiO₂ nanofluid at 3% concentrations is used. It is found that, by replacing water by nanofluid in the bare tube diverter, the heat transfer coefficient is slightly enhanced. In contrast, the swirl-tape insertion considerably enhanced the heat transfer coefficient and this enhancement is considerably increased by replacing water by nanofluid. Although, subcooled boiling is predicted, for bare tube divertor, at incident heat fluxes greater than 10 MW/m² and for swirl-tape inserts tube divertor, at incident heat fluxes greater than 18 MW/m²; nanofluid coolant in the swirl-tape inserts tube divertor remains below the onset of nucleate boiling temperature by a considerable margin (68°C at an incident heat flux of 20 MW/m²).

Nomenclature

a	tube	flow	area (m^2)
а	luoc	110 11	arca (,

c_p specific heat at constant pressure (J/kg°C)

c_p specific heat at con D tube diameter (m)

D_e equivalent hydraulic diameter (m)

D_h equivalent heated diameter (m)

G mass flux (kg/m^2s)

h heat transfer coefficient (W/m² °C)

I enthalpy (J/kg)

I_{fg} latent heat of evaporation (J/kg)

k thermal conductivity (W/m °C)

L active length (m)

Nu Nusselt number $(h D_e/k)$

P pressure (Pa)

Pr Pradentl number $(\mu c_n / k)$

Re Reynolds number (GD_e/μ)

q volumetric heat generation (W/m³)

t temperature (°C)

u coolant velocity (m/s)

v specific volume (m³/kg)

x distance in radial horizontal direction (m)

x steam quality

y distance in radial vertical direction (m)

Y swirl-tape ratio

z distance in axial direction (m)

Greek letters

 α thermal diffusivity (m²/s)

 δ swirl tape thickness (m)

 ρ density (kg/m³)

μ dynamic viscosity (kg/ms)

 σ surface tension (N/m)

 ϕ heat flux (W/m²)

φ nanofluid concentration

Subscripts

c coolant

NCB nucleate boiling contribution

nf nanofluid

ONB onset of nucleate boiling

SP single phase st swirl-tape TP two-phase

REFERENCES

- [1] Draft Report for ITER Concept Definition Phase, IAEA, ITER Technical Report (1989).
- [2] Pitts, R. A., Carpentier, S., Escourbiac, F., Hirai, T., Komarov, V., Lisgo, S., Kukushkin, A.S., Loarte, A., Merola, M., Sashala Naik, A., Mitteau, R., Sugihara, M., Bazylev, B. and Stangeby, P.C., A full tungsten divertor for ITER: physics issues and design status, Journal of Nuclear Materials 438 (2013).
- [3] Hirai, T., Escourbiac, F., Carpentier-Chouchana, S., Durocher, A., Fedosov, A., Ferrand, L., Jokinen, T., Komarov, V., Merola, M., Mitteau, R., Pitts, R. A., Shu, W., Sugihara, M., Barabash, V., Kuznetsov, V., Riccardi, B. and Suzuki, S., ITER full tungsten divertor qualification program and progress, Physica Scripta, T159 (2014).
- [4] Hirai, T., Escourbiac, F., Barabash, V., Durocher, A., Fedosov, A., Ferrand, L., Jokinen, T., Komarov, V., Merola, M., Carpentier-Chouchana, S., Arkhipov, N., Kuznetcov, V., Volodin, A., Suzuki, S., Ezato, K., Seki, Y., Riccardi, B., Bednarek, M. and Gavila, P., Status of technology R&D for the ITER tungsten divertor monoblock Journal of Nuclear Materials 463 (2015).
- [5] Viskanta, R., Critical heat flux for water in swirling flow, Nucl. Sci. Eng. 10 (2) (1961).
- [6] Manglik, R.M., Bergles, A. E., Heat transfer and pressure drop correlations for twisted-tape inserts in isothermal tubes. Part I. Laminar flows, J. Heat Transf. 115 (1993).
- [7] Shatto, D. P., Peterson, G.P., A review of flow boiling heat transfer with twisted tape inserts, J. Enhanc. Heat Transf. 3 (4) (1996).
- [8] Liu, P., Ding, W. L., Ji, J. D., Song, Y. T., Wang, P. T., Peng, X. B., Chen, Q. H., Mao, X., Qian, X. Y. and Zhang, J. W., Heat transfer and thermo-mechanical analyses of W/CuCrZr monoblock divertor in subcooled flow boiling, Fusion Engineering and Design 144 (2019).
- [9] Liu, P., Peng, X. B., Song, Y. T., Fang, X. D., Huang, S. H. and Mao, X., Numerical simulation in a subcooled water flow boiling for one-sidedhigh heat flux in reactor divertor, Fusion Engineering and Design 112 (2016).

- [10] Azmi, W. H., Sharma, K. V., Sarma, P. K., Rizalman Mamat, Shahrani Anuar, Comparison of convective heat transfer coefficient and friction factor of TiO₂ nanofluid flow in a tube with twisted tape inserts, International Journal of Thermal Sciences 81 (2014).
- [11] Azmi, W. H., Sharma, K. V., Sarma, P. K., Rizalman Mamat and Najafi, G., Heat transfer and friction factor of water based TiO₂ and SiO₂ nanofluids under turbulent flow in a tube, International Communications in Heat and Mass Transfer 59 (2014).
- [12] Syam Sundar, L., Ravi Kumar, N. T., Naik, M. T. and Sharma, K. V., Effect of full length twisted tape inserts on heat transfer and friction factor enhancement with Fe₃O₄ magnetic nanofluid inside a plain tube: An experimental study, International Journal of Heat and Mass Transfer 55 (2012).
- [13] Safikhani, H. and Eiamsa-ard, S., Multi-Objective Optimization of Tio2-Water Nanofluid Flow in Tubes Fitted with Multiple Twisted Tape Inserts in Different Arrangement, Trans. Phenom. Nano Micro Scales, 3(2): 89-99, (2015).
- [14] El-Morshedy, S. E. Hassanein, A., Transient thermal hydraulic modeling and analysis of ITER divertor plate system, Fusion Engineering and Design 84 (2009).
- [15] El-Morshedy, S. E. Hassanein, A., Analysis, verification, and benchmarking of the transient thermal hydraulic ITERTHA code for the design of ITER divertor, Fusion Engineering and Design 85 (2010).
- [16] El-Morshedy, S. E., Thermal-hydraulic modelling and analysis of ITER tungsten divertor monoblock, Nuclear Materials and Energy 28 (2021).
- [17] El-Morshedy, S. E., Thermal-hydraulic simulation of ITER tungsten divertor monoblock for loss of flow transient, Nuclear Materials and Energy 38 (2024).
- [18] Ueda, Y., Coenen, J. W., De Temmerman, G., Doerner, R. P., Linke, J., Philipps, V. and Tsitrone, E., Research status and issues of tungsten plasma facing materials for ITER and beyond, Fusion Engineering and Design 89 (2014).
- [19] Panayotis, S., Hirai, T., Barabash, V., Durocher, A., Escourbiac, F., Linke, J., Loewenhoff, Th., Merola, M., Pintsuk, G., Uytdenhouwen, I. and Wirtz, M., Self- castellation of tungsten monoblock under high heat flux loading and impact of material properties, Nucl. Mater. Energy 12 (2017).
- [20] Dittus, F. W. and Boelter, L. M. K., University of California, Berkeley, Publications on Engineering 2 (1930).
- [21] Sieder, E. N. and Tate, G. E., Ind. Eng. Chem. 28 (1429) (1936).
- [22] Maiga, S.B., Nguyen, C. T., Galanis, N., Roy, G., Maré, T. and Coqueux, M., Heat Transfer enhancement in turbulent tube flow using Al₂O₃ nanoparticle suspension. Int. J. Numer. Meth. Heat Fluid Flow. 16 (3) (2006).
- [23] Marshall, T. D., Experimental examination of the post-critical heat flux and loss of flow accident phenomena for prototypical ITER divertor channels, PhD Thesis, Rensselaer Polytechnic Institute, Troy, New York, (1998).
- [24] Lopina, R. F. and Bergles, A. E., Heat transfer and pressure drop in tape-generated swirl flow of single phase water, J. Heat Transf. 91 (8) (1969).
- [25] Timofeeva, E. V., Gavrilov, A. N., McCloskey, J. M. and Tolmachev, Y. V., Thermal conductivity and particle agglomeration in alumina nanofluids: experiment and theory, Phy.Rev. 76 (2007).
- [26] Drew, D. A. and Passman, S. L., Theory of Multi-Component Fluids, Springer, Berlin, (1999).
- [27] . Collier, J. G., Convective Boiling and Condensation, Second edition, Mc Graw-Hill Internal Book Company, (1981).
- [28] Lim, J. H., Park, M., Shin, S. M. and Chung, S. S., New correlations for the prediction of incipient nucleate boiling in a one-side heated swirl tube, Applied Thermal Engineering 209 (2022).
- [29] Chen, J.C., A correlation for Boiling Heat Transfer to Saturated Fluids in Convective Flow, Ind. Eng. Chem. Process Des. Dev. 5 (3) (1966).
- [30] Youa, J. H., Visca, E., Barrett, T., Boswirth, B., Crescenzi, F., Domptail, F., Fursdon, M., Gallay, F., Ghidersa, B. E., Greuner, H., Li, M., Muller, A. V., Reiser, J., Richou, M., Roccella, S. and Vorpahl, Ch., European divertor target concepts for DEMO: Design rationales and high heat flux performance, Nucl. Mater. Energy 16 (2018).
- [31] You, J. H., Copper matrix composites as heat sink materials for water-cooled divertor target, Nucl. Mater. Energy 5 (2015).